Recombination Dynamics and EPR Spectra of the Primary Radical Pair in Bacterila Photosynthetic Reaction Centers with Blocked Electron Transfer to the Primary Acceptor

U. Till,[†] I. B. Klenina,[‡] I. I. Proskuryakov,[‡] A. J. Hoff,[§] and P. J. Hore[†,*]

Physical & Theoretical Chemistry Laboratory, Oxford University, Oxford OX1 3QZ, United Kingdom, Institute of Soil Science and Photosynthesis RAS, Pushchino 142292, Russia, and Department of Biophysics, Huygens Laboratory, Leiden University, 2300 RA Leiden, The Netherlands

Received: February 25, 1997; In Final Form: October 2, 1997[⊗]

Recent electron paramagnetic resonance (EPR) experiments (Proskuryakov, I. I.; Klenina, I. B.; Hore, P. J.; Bosch, M. K.; Gast, P.; Hoff, A. J. *Chem. Phys. Lett.* **1996**, *257*, 333) on the primary radical pair in bacterial reaction centers are interpreted in detail. The spin-correlated radical pair model is extended to include the time dependence of the EPR intensities, differential lifetime broadening of the basic four-line spectrum, and averaging over the inhomogeneous distributions of hyperfine interactions in the two radicals. Values of the singlet and triplet recombination rate constants and the magnitude and sign of the exchange interaction of the radical pair are obtained from the shape and linewidth of the spin-polarized EPR spectra and the kinetics of formation of the triplet state of the primary electron donor. For *Rhodobacter sphaeroides* at 70 K, $k_S = (1.2 \pm 0.3) \times 10^7$ s^{-1}, $k_T = (5.7 - 8.8) \times 10^8$ s^{-1}, $-J = 8 - 6$ G; and for *Rhodopseudomonas viridis* at 190 K, $k_S = (8 \pm 2) \times 10^7$ s^{-1}, $k_T = (6.5 - 10.0) \times 10^8$ s^{-1}, $-J = 17 - 16$ G. The reliability of these values is discussed in the light of the energetic heterogeneity of the radical pair energies (Ogrodnik, A.; Keupp, W.; Volk, M.; Aumeier, G.; Michel-Beyerle, M. E. *J. Phys. Chem.* **1994**, *98*, 3432−3439) and of the sensitivity and selectivity of the EPR measurements toward the three parameters.

1. Introduction

The light-induced electron transfer processes in bacterial photosynthetic reaction centers are controlled by the energies of the various donor and acceptor molecules involved.[1−6] These energies may be determined from the recombination dynamics of the radical pairs formed by charge separation and from the exchange interactions of the unpaired electrons in the radicals.[7] Such information is available from a variety of experiments, including the effects of static magnetic fields on radical pair lifetimes and recombination product yields;[8−11] from RYDMR (reaction yield detected magnetic resonance);[12−16] and from the electron spin polarization of the reduced primary acceptor, Q_A^-, a semiquinone,[17−19] and of the secondary radical pair $P^+Q_A^-$.[20] However, these experiments provide at best indirect information on the exchange interaction J in the primary radical pair $P^+\Phi_A^-$ formed from the primary electron donor P, a bacteriochlorophyll dimer, and the bacteriopheophytin acceptor, Φ_A. The magnitude and sign of J are important in theoretical attempts to describe the kinetics and energetics of electron transfer in photosynthetic reaction centers.[21,22]

Very recently, a much more direct source of information on the exchange interaction of P^+ and Φ_A^- has become available in the form of EPR (electron paramagnetic resonance) detection of $P^+\Phi_A^-$ under conditions where forward electron transfer is blocked by removal or chemical reduction of the primary acceptor Q_A.[23] A new transient EPR signal with g-value close to 2 was found, with AE polarization (absorptive at low field, emissive at high field), and peak-to-peak separations of ∼38.5 G in *Rhodobacter* (*Rb.*) *sphaeroides* and ∼68 G in *Rhodopseudomonas* (*Rps*) *viridis*. In both cases, the triplet state of the primary donor ^{3}P was formed with first order kinetics,

SCHEME 1

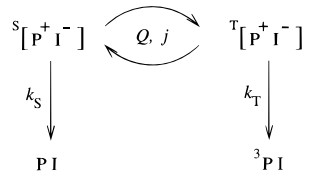

with time constants at 70 K of 38 ns for Q_A-reduced *Rb. sphaeroides*, ∼53 ns for Q_A-removed *Rb. sphaeroides* and ∼10 ns for Q_A-reduced *Rps. viridis*. In Q_A-removed *Rb. sphaeroides*, the ^{3}P spectrum was found to grow at the same rate as the new signal disappeared, providing strong support for the assignment of the new signal to the radical pair precursor of ^{3}P. A preliminary analysis of the EPR spectra, using the so-called spin-correlated radical pair model (SCRP),[18,24−26] gave rough estimates of the rate constant for the recombination of the triplet radical pair and for the exchange and dipolar couplings in $P^+\Phi_A^-$.

Here, we adapt and extend the theory of radical pair EPR spectra by including the effects of rapid recombination and large electron spin−spin interactions, so as to interpret the spectra in more detail. We also analyse the kinetics of formation of ^{3}P in terms of the dynamics of the singlet−triplet mixing in the radical pair and the spin-selective recombination reactions. Values of the singlet and triplet recombination rates and the magnitude and sign of J are obtained.

2. Kinetics of ^{3}P Formation

Theory. The steps leading to the production of the triplet state of the primary donor are outlined in Scheme 1. The radical pair is formed in a singlet state, which undergoes coherent singlet−triplet interconversion driven by hyperfine and Zeeman interactions and hindered by the exchange and dipolar coupling of the two electron spins. In a strong magnetic field the $T_{\pm1}$ states of $P^+\Phi_A^-$ are energetically isolated by the Zeeman interaction, so that only the T_0 triplet level becomes populated.

* To whom correspondence should be addressed. Email: hore@physchem.ox.ac.uk.
† Oxford University.
‡ Institute of Soil Science and Photosynthesis RAS.
§ Leiden University.
⊗ Abstract published in *Advance ACS Abstracts,* December 1, 1997.

S1089-5647(97)00686-X CCC: $14.00

Recombination is possible from both singlet and triplet states of $P^+\Phi_A^-$ to give, respectively, P in its ground state and the triplet ^3P, with rate constants k_S and k_T.[27,28] The parameters that characterize the evolution of the radical pair are thus k_S and k_T, the singlet−triplet mixing frequency $2Q$ (which is the difference in Larmor frequencies of the two electrons in the absence of spin−spin interactions), and the spin−spin interaction $2j$ (the singlet−triplet energy gap when $Q = 0$), which has contribution from exchange (J) and dipolar (D) couplings:[18]

$$j = J + {}^1/_2D(\cos^2\xi - {}^1/_3) \quad (1)$$

ξ is the angle between the magnetic field and the dipolar axis.

An exact analytical solution of the stochastic Liouville equation that describes the time dependence of the system has recently been published.[28] The concentration of triplet radical pairs formed from a nondiffusing, nonrelaxing, initially singlet spin-correlated pair in a strong static magnetic field is shown to be the sum of four time-dependent terms: two decaying exponentials and two exponentially damped oscillations,

$$[^3RP]_t = A\{\exp[-\lambda_1 t] + \exp[-\lambda_2 t] + \exp[-(\lambda_3+i\mu)t] + \exp[-(\lambda_3-i\mu)t]\} \quad (2)$$

in which the three rate constants λ_1, λ_2, λ_3, the oscillation frequency μ, and the amplitude A are all functions of k_S, k_T, Q, and j. All four quantities have roughly comparable values for $P^+\Phi_A^-$ in photosynthetic bacteria (in the range 10^7-10^9 s^{-1}) so that the singlet−triplet interconversion and the recombination occur on a similar timescale, prohibiting any simplification of eq 2. For typical values of k_S, k_T, Q, and j, three of the terms in eq 2 are damped much more rapidly than the fourth,[28] such that by about 20 ns after the creation of the pair only the slower nonoscillatory exponential decay has appreciable amplitude. However, this only results in monoexponential kinetics for unique values of Q and j. In reality, Q has an inhomogeneous distribution arising principally from the variety of possible nuclear spin configurations and, therefore, hyperfine interactions, in the two radicals, but also from g-anisotropy; similarly the dipolar interaction between the two electron spins leads to an appreciable anisotropy in j. As a consequence the decay of the triplet radical pair is not monoexponential, even for times after ~20 ns.[7,28,29] Such deviations from first-order kinetics have been detected experimentally.[7]

The time dependence of the amount of ^3P is calculated from eq 2 via

$$[^3P]_t = k_T \int_0^t [^3RP]_{t'}\, dt' \quad (3)$$

followed by integration over the distribution of local hyperfine fields in the two radicals and, if anisotropic interactions are included, over all orientations of the pair with respect to the static field. The former is achieved using a Gaussian distribution for Q with a width (8.14 G) determined by the Gaussian line widths of the EPR spectra of P^+ [30] and Φ_A^- [31] (i.e., ${}^1/_2[(9.8)^2 + 13.0^2]^{1/2}$), and a mean, $\langle Q\rangle$, determined by the difference in Zeeman interactions of the two electrons. For X-band EPR, taking the g-tensors to be isotropic with $\Delta g = 0.001$,[30,31] $\langle Q\rangle$ equals 0.825 G.

***Rhodobacter sphaeroides* R26.** The kinetics of formation of ^3P were calculated as described above. For representative values of the recombination rate constants ($k_S \simeq (1 \times 10^6)-(2 \times 10^7)$ s^{-1}, $k_T \simeq 10^8 - 10^9$ s^{-1}) and the exchange interaction, $|J| \simeq 2-10$ G, ^3P should be formed with *approximately* first order kinetics, as discussed in ref 28. Figure 1 shows the effective time constant τ_{eff} for this process, obtained from the average gradient of a plot of $\ln([^3P]_{t=\infty} - [^3P]_t)$ against time in the interval 100−200 ns. As the figure demonstrates, τ_{eff} decreases appreciably as k_S is increased, but is almost independent of k_T and $|J|$ in the ranges studied. The anisotropic (dipolar) part of the electron−electron coupling was also found to have a negligible effect on the triplet kinetics, for $-15 < D < 0$ G. The dipolar parameters of a radical pair is expected to be *negative*: positive values were therefore not explored.

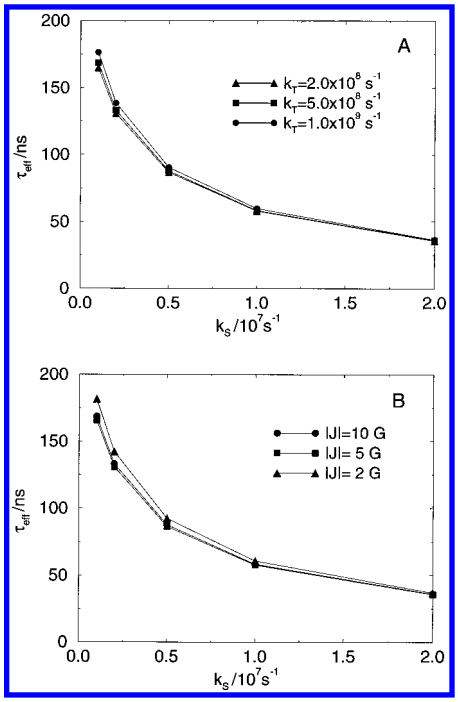

Figure 1. Dependence of the effective time constant τ_{eff} for the formation of ^3P on the singlet recombination rate constant k_S, for various values of the triplet recombination rate constant k_T and the exchange interaction J. Anisotropic interactions in the radical pair are omitted. The τ_{eff} values have been averaged over a Gaussian distribution of the singlet−triplet mixing parameter Q with width 8.14 G and mean 0.825 G. (A) $|J| = 5$ G, $k_T = 1.0 \times 10^9$ s^{-1} (●), 5.0×10^8 s^{-1} (■), 2.0×10^8 s^{-1}, (▲). (B) $k_T = 5.0 \times 10^8$ s^{-1}, $|J| = 10$ G, (●); 5 G (■), 2 G (▲).

At first sight the lack of dependence of τ_{eff} on k_T and J is surprising, because both quantities have a profound effect on the distributions of time constants for the production of ^3P (Figure 2A). These distributions span the range from $\tau = [{}^1/_2(k_S + k_T)]^{-1}$ to $\tau = k_S^{-1}$: the larger the singlet−triplet mixing frequency $2Q$, the shorter the radical pair lifetime.[7,28] To understand the behavior in Figure 1, one has to remember that the timespan (>100 ns) over which τ_{eff} is measured[23] and calculated, is such that only the slowest contributions to the overall kinetics are detected. The five curves in Figure 2A have remarkably similar shape in the $\tau \gtrsim 40$ ns region (emphasized in Figure 2A by the use of different vertical scalings), and therefore lead to values to τ_{eff} that are almost independent of k_T and J. That these distributions actually have different amplitudes for $\tau \gtrsim 40$ ns simply affects the intensity of the EPR signals, not their time dependence. In contrast (Figure 2B), the shape of this long lifetime region of the distribution varies markedly with k_S, in agreement with Figure 1. The difference from Figure 2A clearly arises because the longest time constant in the system is determined by k_S and not by k_T.

The observed rise time of the ^3P EPR signal is evidently a good measure of k_S, more-or-less independent of the values assumed for k_T, J, and D. Taking the experimentally observed time constant for the formation of ^3P in quinone-depleted *Rb.*

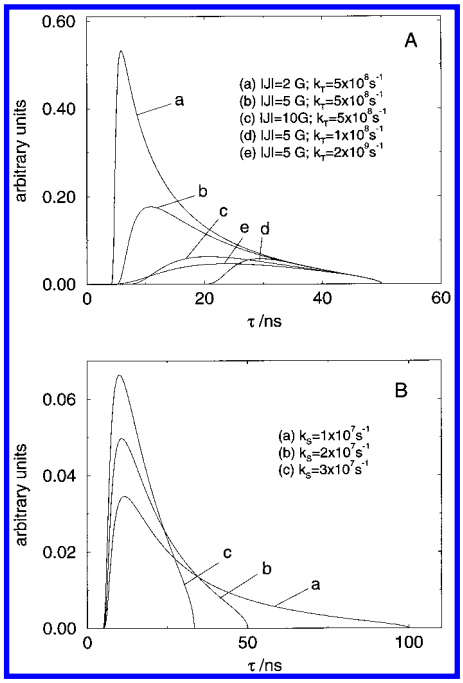

Figure 2. Distributions of time constants τ for the formation of ^{3}P from $P^+\Phi_A^-$. (A) Scaled distributions for $k_S = 2 \times 10^7$ s^{-1}: (curve a) $|J| = 2$ G, $k_T = 5 \times 10^8$ s^{-1}; (curve b) $|J| = 5$ G, $k_T = 5 \times 10^8$ s^{-1}; (curve c) $|J| = 10$ G, $k_T = 5 \times 10^8$ s^{-1}; (curve d) $|J| = 5$ G, $k_T = 1 \times 10^8$ s^{-1}; (curve e) $|J| = 5$ G, $k_T = 2 \times 10^9$ s^{-1}. (B) Normalized distributions for $|J| = 5$ G, $k_T = 5 \times 10^8$ s^{-1}: (curve a) $k_S = 1 \times 10^7$ s^{-1}, (curve b) $k_S = 2 \times 10^7$ s^{-1}, (curve c) $k_S = 3 \times 10^7$ s^{-1}. These distributions arise from the range of possible singlet−triplet mixing frequencies: the extremes are $\tau = k_S^{-1}$ (slow mixing) and $\tau = [^1/_2(k_S + k_T)]^{-1}$ (fast mixing). The five distributions in A have been individually scaled to reveal most clearly the similarity of their shapes in the $40 < \tau < 50$ ns region. The curves in B have been normalized so as to have equal areas.

sphaeroides R26 at 70 K[23] with an estimated error of 10% (i.e., $\tau_{eff} = 53 \pm 5$ ns), one obtains from Figure 1 a value for k_S of $(1.2 \pm 0.3) \times 10^7$ s^{-1}.

Rhodopseudomonas viridis. A procedure similar to the above may be used to estimate k_S in *Rps. viridis* from the observed time constant for ^{3}P formation (~10 ns at 70 K for Q_A-reduced samples[23]). As in the case of *Rb. sphaeroides*, we found that τ_{eff} was almost independent of k_T in the range $(10 \pm 5) \times 10^8$ s^{-1}. However, the larger values of J needed to account for the EPR spectrum of $P^+\Phi_A^-$ (see below) had a noticeable effect on k_S. With $|J|$ in the range 15 ± 2 G, we estimate $k_S = (8 \pm 2) \times 10^7$ s^{-1}. That this value is substantially larger than the 1.2×10^7 s^{-1} found above for *Rb. sphaeroides* principally reflects the much faster formation of ^{3}P observed for *Rps. viridis*. A larger singlet recombination rate constant is also required to compensate for the slower singlet−triplet interconversion brought about by the stronger exchange interaction in *Rps. viridis*.

3. Electron Paramagnetic Resonance Spectra of $P^+\Phi_A^-$

Spin-Correlated Radical Pair Model. Our interpretation of the spin-polarized EPR spectra of the primary radical pair $P^+\Phi_A^-$ is based on the so-called SCRP model used extensively to interpret the spectra of the secondary radical pair $P^+Q_A^-$ in both plants and bacteria.[18,24−26] We first summarize the salient features of the SCRP approach as it is applied to $P^+Q_A^-$.

Radical pairs are formed in a spin-correlated singlet state, which, when projected onto the electron spin eigenstates of the two coupled electrons in a strong magnetic field, leads to the

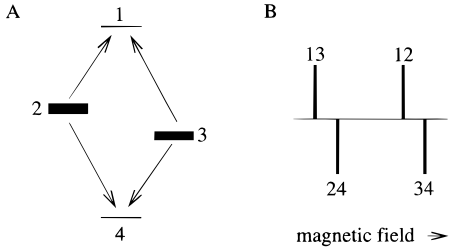

Figure 3. Energy levels A and schematic spectrum B of a spin-correlated radical pair created from a singlet precursor. The thickness of the energy levels indicates their initial populations. The spectrum has been drawn for a negative exchange interaction ($J < 0$) with no dipolar coupling ($D = 0$). The spin eigenstates and EPR frequencies are given by eqs 6 and 10, respectively.

population of two of the states (2 and 3, see Figure 3A), according to their singlet character, leaving the other two (1 and 4), which are pure triplet, empty. This selective population of the eigenstates of the pair leads to polarized EPR spectra, which, for isolated electron spins, comprise two antiphase doublets whose splittings are determined by the electron−electron spin−spin coupling (Figure 3B). This prototype spectrum has a center of inversion symmetry, and all four transitions have equal (absorptive or emissive) intensity. To calculate spectra for randomly oriented reaction centers, the four-line spectrum is spherically averaged, including *g*-anisotropy and electron−electron dipolar interactions, and then convolved with a Gaussian line broadening to mimic the effect of unresolved hyperfine couplings and the natural linewidth due to spin relaxation. Below 100 K, the lifetime of $P^+Q_A^-$ with respect to charge recombination is 30 ms in *Rb. sphaeroides* and 9 ms in *Rps. viridis*,[32] so that the reactivity of the pair can safely be ignored on the time scale of its observation by EPR (~1 μs).[20,33,34] A further simplification is to ignore the electron−electron zero-quantum (ZQ) coherence which is created when the pair is formed.[35] Although zero-quantum oscillations have been observed in photosynthetic radical pairs,[36−39] they rapidly dephase and relax and are not expected to be visible in the experiments discussed here (see below).

Theory of Spin-Polarized $P^+\Phi_A^-$. $P^+\Phi_A^-$ differs from $P^+Q_A^-$ in two important respects. First, recombination from both singlet and triplet states occurs on a time scale comparable to that of the EPR measurement (~100 ns). Second, both the dipolar coupling and, especially, the exchange interaction are stronger: in contrast to $P^+Q_A^-$ they are both *larger* in $P^+\Phi_A^-$ than the root mean square value of Q.

The faster recombination has two consequences, the first being that the eigenstate populations can no longer be regarded as independent of time. If the two rate constants k_S and k_T were *equal* (say to k), one would simply multiply the populations of states 2 and 3, and therefore the amplitudes of all four EPR lines, by $\exp(-kt)$.[28] However, k_S and k_T differ by more than an order of magnitude,[7] and states 2 and 3, which have different singlet character, will in general be depopulated at different rates, depending on Q and j, as well as k_S and k_T. The four contributions to the basic spectrum (Figure 3B) will therefore no longer be of equal magnitude.

Ignoring the ZQ coherence, the EPR intensities may be calculated from the matrix elements of the density operator of the radical pair $\rho(t)$ in the singlet−triplet (S, T_0) basis[18]

$$I_{12} = -I_{24} = {}^1/_2[c^2\rho_{SS} + s^2\rho_{TT} + cs(\rho_{ST} + \rho_{TS})]s^2$$

$$I_{13} = -I_{34} = {}^1/_2[s^2\rho_{SS} + c^2\rho_{TT} - cs(\rho_{ST} + \rho_{TS})]c^2 \quad (4)$$

where

$$c = \cos\psi, \quad s = \sin\psi; \quad \tan 2\psi = Q/j \tag{5}$$

Exact general expressions for the four density matrix elements, in terms of Q, j, k_S, and k_T, are taken from ref 28. The outcome is that the inner pair of lines (12 and 24 in Figure 3B) become weaker than the outer pair. Omission of the ZQ contributions to eq 4 is justifiable on the basis of similar experiments on $P^+Q_A^-$ in which the quantum beats disappear very quickly.[36−39] ZQ dephasing will be even faster in $P^+\Phi_A^-$ because of the larger dipolar interaction which produces a greater dispersion in the ZQ oscillation frequency. Further, there is no suggestion of oscillatory components in the detected EPR signals.[23] The matrix elements of ρ in eq 4, as given in ref 28, are time-dependent as a result of singlet−triplet intercoversion and recombination reactions. Although in principle the relative intensities of the inner and outer EPR lines should vary, the effect turns out to be small (see Figure 2 of ref 28). Since the triplet radical pairs recombine roughly an order of magnitude faster than the singlets, the expressions in eq 4 are dominated by ρ_{SS}, so that $I_{12}/I_{13} \cong \cot^2\psi$. The simulations reported below, of experimental spectra averaged over the interval $100 < t < 200$ ns, use eq 4 with $t = 150$ ns.

The second consequence of the rapid recombination of $P^+\Phi_A^-$ is that lifetime broadening of the EPR transitions must be included. Once again we can anticipate different effects on states 2 and 3 because of their different singlet and triplet characters. A state depopulated with a rate constant k has a Lorentzian broadening of $k/2\pi$ Hz, so that a transition between two such states has a Lorentzian width of k/π Hz; this is the familiar magnetic resonance line broadening in the slow exchange regime. Now, since the four eigenstates are[24,25]

$$\begin{aligned} |1\rangle &= |T_{+1}\rangle \\ |2\rangle &= c|S\rangle + s|T_0\rangle \\ |3\rangle &= -s|S\rangle + c|T_0\rangle \\ |4\rangle &= |T_{-1}\rangle \end{aligned} \tag{6}$$

their Lorentzian widths are

$$\begin{aligned} \Delta\nu_1 &= k_T/2\pi \\ \Delta\nu_2 &= [c^2k_S + s^2k_T]/2\pi \\ \Delta\nu_3 &= [s^2k_S + c^2k_T]/2\pi \\ \Delta\nu_4 &= k_T/2\pi \end{aligned} \tag{7}$$

and the four transitions have line broadenings

$$\begin{aligned} \Delta\nu_{12} = \Delta\nu_{24} &= [c^2k_S + (s^2{+}1)k_T]/2\pi \\ \Delta\nu_{13} = \Delta\nu_{34} &= [s^2k_S + (c^2{+}1)k_T]/2\pi \end{aligned} \tag{8}$$

Thus, in general, the inner lines are broader than the outer lines, and the line shape is Lorentzian in contrast to the Gaussian convolution used to model the homogeneous and inhomogeneous broadening of $P^+Q_A^-$.[24,26]

The other difference between $P^+Q_A^-$ and $P^+\Phi_A^-$ mentioned above is the larger spin−spin coupling in the latter, which means that the two electron spins are much more likely to be strongly coupled, in the sense that the doublet splitting is comparable to or larger than the difference in Larmor frequencies of the two electron spins. As a result, it is no longer a good approximation to introduce the hyperfine couplings by means of a Gaussian convolution of the whole spectrum.[24,26] Rather, one should sum the basic four-line spectra over a distribution of resonance frequencies of the two electrons ω_P and ω_I, the appropriate distributions being the EPR line shapes of the two isolated radicals. Thus ω_P and ω_I are given Gaussian distributions with widths 9.8 and 13.0 G respectively,[30,31] affecting both the center of the spectrum ω and the singlet−triplet mixing parameter Q

$$\omega = {}^1/_2[\omega_P + \omega_I], \quad Q = {}^1/_2[\omega_P - \omega_I] \tag{9}$$

In summary, the differences between our treatment of $P^+\Phi_A^-$ and the standard SCRP model of $P^+Q_A^-$[18,24−26] are 3-fold. The four EPR intensities are time-dependent functions of k_S and k_T as well as Q and j; the inner and outer lines have different widths, also depending on Q, j, k_S, and k_T; and the basic four-line pattern must be averaged over the inhomogeneous distributions of ω_P and ω_I, as well as over all orientations. The small extra line width arising from spin relaxation is much smaller than the lifetime broadening and is ignored.

Appearance of Spectra. Before discussing the simulated spectra of $P^+\Phi_A^-$, it is instructive to consider what the spectra should look like in the limit that the spin−spin coupling $|2J|$ is much larger than the difference in the two Larmor frequencies $|2Q|$ for all values of ω_P and ω_I. It is easily seen from the expressions for the frequencies of the four transitions[24,25] (omitting the dipolar contribution to j):

$$\begin{aligned} \omega_{12} &= \omega - \Omega - J \\ \omega_{34} &= \omega - \Omega + J \\ \omega_{13} &= \omega + \Omega - J \\ \omega_{24} &= \omega + \Omega + J \end{aligned} \tag{10}$$

that, for $J < 0$, the two inner lines (12 and 24 in Figure 3) are nearly degenerate, and therefore almost cancel one another, while the two outer lines (13 and 34) are shifted from the center of the spectrum by $\pm 2J$:

$$\begin{aligned} \Omega = [Q^2 + J^2]^{1/2} &\simeq |J| \\ \omega_{34} &\simeq \omega + 2J \\ \omega_{12} \simeq \omega_{24} &\simeq \omega \\ \omega_{13} &\simeq \omega - 2J \end{aligned} \tag{11}$$

This cancellation should be particularly effective because, as described above, the inner lines are both weaker and broader than the outer pair.

Hence, in the strong coupling limit, we can anticipate a spin-polarized spectrum comprising two oppositely polarized lines, with peak-to-peak separation $\Delta B_{pp} \simeq |4J|$ and approximate inversion symmetry, provided the g-anisotropy is not too large. However, this will only be observed if the lifetime broadening is strong enough to ensure that the inner lines cancel and not so large as to cause the outer lines to overlap significantly with one another. In the latter case, ΔB_{pp} can be expected to be larger than $|4J|$. For positive J, the low-field part of the spectrum is in emission and the high-field part absorption (denoted EA). The effect of changing the sign of J is simply to invert the whole spectrum (to AE).

Additionally, one can see from eqs 8 that, in the strong coupling limit, the two outer lines have width $(k_S + k_T)/2\pi$ which is approximately $k_T/2\pi$ if $k_T \gg k_S$. This is half the width that would normally be expected for a radical disappearing with rate constant k_T, because both of these transitions link a pure triplet state (1 or 4), which has a frequency uncertainty of $k_T/2\pi$, with a state which is essentially pure singlet of negligible width ($k_S/2\pi$).

At first sight, strong coupling would appear to be a poor approximation for a sizeable fraction of the radical pairs because the root mean square value of Q (~4 G) is only slightly smaller than generally accepted values of $|J|$ (5−10 G) and D (−5 G). However, the EPR experiments under consideration are not uniformly sensitive to all values of Q. Radical pairs with large Q experience fast singlet−triplet interconversion, recombine rapidly to ^{3}P, and make only a small contribution to the kinetics observed after 100 ns. Therefore we can expect the EPR signal to come principally from radical pairs with relatively small Q and slow singlet−triplet mixing, for which the strong coupling limit is reasonably accurate. This conclusion is consistent with the discussion of Figure 1, in which it was seen that only radical pairs with small Q, and therefore large τ, make a strong contribution to τ_{eff}. Note that the strong coupling approximation is introduced here *only* to facilitate understanding of the appearance of the spectra. The approximation is *not* employed in the calculations discussed below, which were all performed using the exact forms of eqs 4−9.

Rb. sphaeroides R26. The observed EPR spectrum of *Rb. sphaeroides* R26 at 70 K, averaged over the interval 100−200 ns after the formation of $P^+\Phi_A^-$[23] is shown in Figure 4 together with several spectra simulated as described above. The singlet recombination rate was kept fixed at 1.2×10^7 s^{-1} (see section 2); k_S has very little effect on the shape of spectra in the range $(1.0 \times 10^7) - (1.0 \times 10^8)$ s^{-1}, although it does have a profound influence on their amplitude through its effect on the kinetics of ^{3}P formation. Inclusion of the dipolar interaction between P^+ and Φ_A^-, calculated to be −4.8 G from the X-ray structure[40] using a point dipole approximation, as well as the *g*-anisotropy of P^+,[41] had no perceptible effect on the spectra. Provided J is *negative*, the spectra are all AE polarized.

The *g*-anisotropy of Φ_A^- is not yet reliably known, but can be expected to be roughly comparable to that of P^+ (~0.001). Spectra calculated using a variety of *g*-tensors for Φ_A^- were imperceptibly affected when realistic values of the anisotropy (≤0.005) were introduced. Given the strong lifetime broadening and dominant effect of the isotropic exchange interaction, it is not surprising that small anisotropic interactions have a negligible influence of the spectra.

Increasing the triplet recombination rate constant (Figure 4A) broadens the spectrum, pushing the peaks apart and boosting the intensity of the wings. Increasing the exchange interaction (Figure 4B) has a somewhat similar effect, leading eventually to a weak flat region in the center of the spectrum where the inner pair of lines would be if they had not cancelled one another, as discussed above. From these simulations it is clear that the observed peak-to-peak separation ($\Delta B_{pp} \simeq 38.5$ G) *alone* is not sufficient to determine k_T and J uniquely. For example, if one chooses $J = -5$ G, as found from RYDMR in the temperature range 95−165 K,[7] then $k_T = 9.5 \times 10^8$ s^{-1} is required to reach a 38.5 G separation. Interestingly, this is very close to the value obtained when the RYDMR data for k_T[7] are extrapolated from 95−165 K down to 70 K, the temperature at which the EPR spectrum was measured. However, this large recombination rate gives such extreme lifetime broadening that the calculated wings of the spectrum are too intense (Figure 4A). Alternatively, if one takes $J = -9$ G, as we did in our preliminary analysis of these data,[23] one needs $k_T = 4.0 \times 10^8$ s^{-1}, and now the wings are too weak (Figure 4B). The best compromise is $k_T = (5.7-8.8) \times 10^8$ s^{-1}, $-J = 8-6$ G, see Figure 4C; these parameters reproduce the experimental spectrum very satisfactorily. In agreement with the experimental observations,[23] the amplitude of this spectrum decays approximately exponentially, with a time constant close to 53 ns.

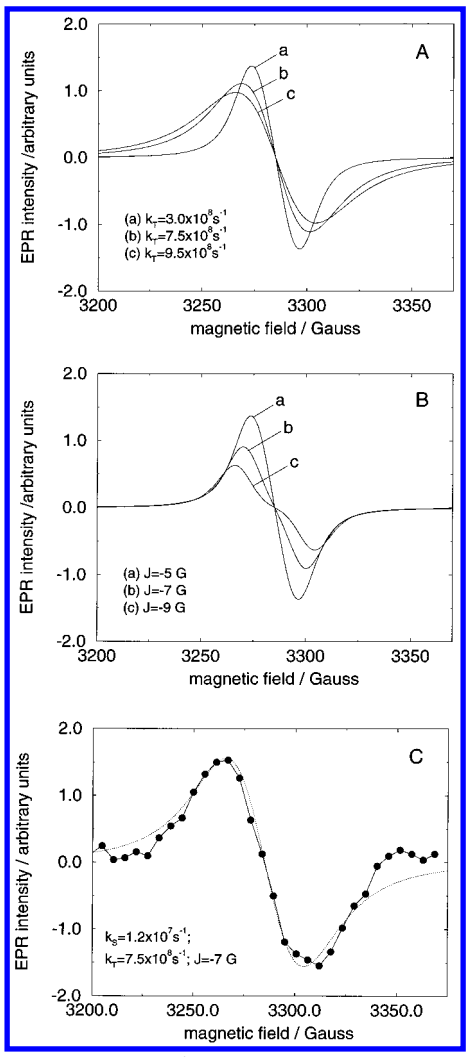

Figure 4. EPR spectra of $P^+\Phi_A^-$ in *Rb. sphaeroides*. (A) Simulated spectra: (curve a) $k_S = 1.2 \times 10^7$ s^{-1}, $J = -5$ G, and (curve a) $k_T = 3.0 \times 10^8$ s^{-1}; (curve b) $k_T = 7.5 \times 10^8$ s^{-1}; (curve c) $k_T = 9.5 \times 10^8$ s^{-1}. (B) Simulated spectra: (curve a) $k_S = 1.2 \times 10^7$ s^{-1}, $k_T = 3.0 \times 10^8$ s^{-1}, and (curve a) $J = -5$ G; (curve b) $J = -7$ G; (curve c) $J = -9$ G. (C) Experimental[23] (circles) and simulated spectra (dotted line): $k_S = 1.2 \times 10^7$ s^{-1}, $k_T = 7.5 \times 10^8$ s^{-1}, $J = -7$ G. The *g*-values used for the simulations were $g_P = 2.0026$, $g_I = 2.0036$.

Rps viridis. The EPR spectrum of $P^+\Phi_A^-$ in *Rps. viridis* at 190 K[23] resembles that of *Rb. sphaeroides* at 70 K: an AE-polarized line with an approximate center of symmetry, Figure 5. The *Rps. viridis* spectrum, however, is broader and shows slight but reproducible shoulders between the two extrema, indicated by asterisks.

The spectra calculated for *Rps. viridis* have similar properties to those found above for *Rb. sphaeroides*. In particular, J and k_T have parallel effects on the peak-to-peak separation ΔB_{pp} (Figure 6). Although the experimental value of 68 G can be reproduced with, for example, $J = -13$ G and $k_T = 1.5 \times 10^9$ s^{-1}, such a large recombination rate constant gives far too much intensity in the wings of the spectrum A reasonable agreement between simulation and experiment (Figure 5) is obtained for

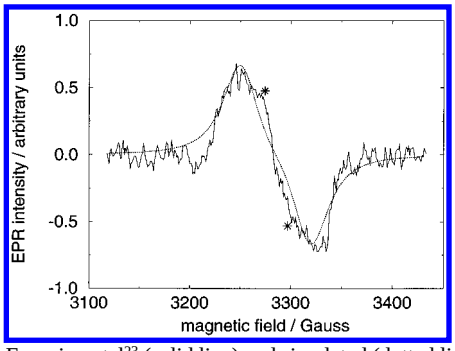

Figure 5. Experimental[23] (solid line) and simulated (dotted line) spectra of $P^+\Phi_A^-$ in *Rps. viridis*. $J = -17$ G, $k_T = 6.5 \times 10^8$ s^{-1}, $k_S = 8 \times 10^7$ s^{-1}, $D = 0$. The same distribution of Q values was used as for *Rb. sphaeroides* R26 (Figure 4). Asterisks indicate the shoulders discussed in the text.

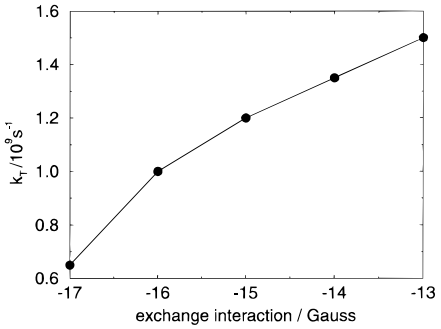

Figure 6. Values of the parameters J and k_T that give a simulated peak-to-peak separation of 68 G for $P^+\Phi_A^-$ in *Rps. viridis*. As described in the text, the graph is insensitive to D and k_S; the values used here are 0 and 8×10^7 s^{-1}, respectively.

$-J = 17-16$ G, $k_T = (6.5-10.0) \times 10^8$ s^{-1}, for which ΔB_{pp} is roughly $|4J|$, as discussed above. Larger values of $|J|$ gives peak-to-peak separations that exceed 68 G, whatever the value of k_T.

Although the simulations satisfactorily reproduce the overall shape and width of the spectrum, at no point was there any suggestion of the fine structure observable in the experimental spectrum. A potential source of this structure is the dipolar coupling between the radicals, which was omitted from the simulations in Figure 5. Inclusion of the −4.8 G dipolar interaction calculated from the center-to-center separation of $P^+\Phi_A^-$ [40] makes no perceptible difference to the simulations. Changing D to −30 G reduces ΔB_{pp} by about 9 G, without much change in the line shape. However, for $D \lesssim -40$ G, shoulders start to appear on the *outer* slopes of the AE spectrum, in contrast to the experimental spectrum which has shoulders *between* the peaks. Despite extensive searches of the parameter space, we were unable to find a combination of D, J, and k_T that reproduced these features. The singlet recombination rate k_S has no effect on the shape of the simulated spectrum provided it is less than about 20% of k_T, as found for *Rb. sphaeroides*.

***Rb. sphaeroides* YW(M210) Mutant.** The YW(M210) mutant of *Rb. sphaeroides* (prepared as described in ref 42) gives a more structured $P^+\Phi_A^-$ spectrum than either *Rb. sphaeroides* R26 or *Rps. viridis*. It still has approximate inversion symmetry, but now the pattern of polarization in AAEE (Figure 7). The outer pair of AE peaks are separated by ∼96 G, and the inner pair by ∼30 G.

It was found to be impossible to simulate such a lineshape using the model described above, even with very large dipolar interactions. For $k_T \lesssim 6 \times 10^8$ s^{-1}, the lifetime broadening is small enough that the inner lines of the basic four-line pattern become visible, but these have the opposite polarization to the corresponding outer lines (see Figure 3), giving an AEAE rather than an AAEE pattern.

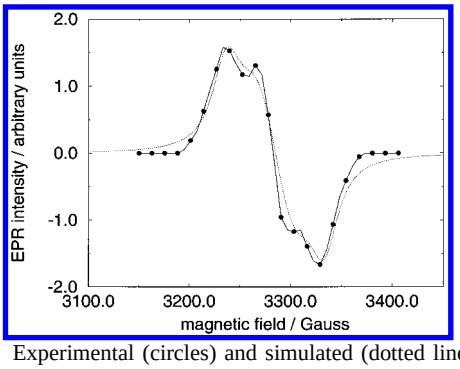

Figure 7. Experimental (circles) and simulated (dotted line) spectra of $P^+\Phi_A^-$ in the YW(M210) mutant of *Rb. sphaeroides* at 30 K. The simulation is the sum of two spectra: $J = -24$ G, and $J = -9$ G, with relative weights 1.00:0.15 respectively. $k_S = 1.2 \times 10^7$ s^{-1}, $k_T = 5 \times 10^8$ s^{-1}, $D = 0$. The same distribution of Q values was used as for *Rb. sphaeroides* R26 (Figure 4).

The experimental spectrum has the *appearance* of two superimposed spectra of the type observed for native *Rb. sphaeroides* R26, with the peak-to-peak separations mentioned above. On this basis, it proved straightforward to obtain respectable (but not exact) simulations: for example, Figure 7 shows a 1.00:0.15 combination of spectra with $J = -24$ G and $J = -9$ G. The latter contribution makes a disproportionate contribution because of its smaller $|J|$ (cf. Figure 4).

4. Discussion

Dipolar Interactions in $P^+\Phi_A^-$. In our preliminary discussion of the EPR spectra of *Rb. sphaeroides* R26 and *Rps. viridis*,[23] using the unmodified $P^+Q_A^-$ SCRP model, we found that the spectrum of the former could be satisfactorily simulated with dipolar interactions in the range −30 to +15 G (*not* −30 ± 15 G, as stated erroneously in Table 1 of ref 23). By contrast, the spectrum of *Rps. viridis*, which displays weak shoulders superimposed on a line that is broader than, but otherwise similar to, that of *Rb. sphaeroides*, could be reproduced using the same model, with $D = -30 \pm 5$ G.[23] Without a dipolar coupling of this magnitude, no shoulders appeared in the simulated spectra.

The more sophisticated analysis described here, using an extended SCRP model, confirms that the *Rb. sphaeroides* spectrum contains no information on the magnitude of D. But it proved impossible to reproduce either the fine structure in the *Rps. viridis* spectrum, or the much more pronounced structure observed for the YW(M210) mutant of *Rb. sphaeroides*, using dipolar couplings in the range $0 \geq D \geq -40$ G.

The dipolar coupling constant in $P^+\Phi_A^-$ can be calculated from the spin densities in the two radicals and the X-ray structure of the reaction center, on the assumption that the charge separated state $P^+\Phi_A^-$ has the same geometry as the electronic ground state $P\Phi_A$. The simplest approach is to use a point dipole approximation:

$$D = (-2.78 \times 10^4)R^{-3} \qquad (12)$$

in which R is the separation of the two magnetic moments in Å, and D is in Gauss. The center-to-center distances between P and Φ_A in *Rb. sphaeroides*[40] and *Rps. viridis*[43] are respectively 18.1 and 17.8 Å, giving $D = -4.7$ and −4.9 G.

The unpaired electron in P^+ is known to be unevenly distributed over the two halves of the special pair dimer, P_L and P_M, with twice as much spin density on the L-half than the M-half.[44] The center-to-center distances in *Rb. sphaeroides* from Φ_A to P_L and P_M are rather similar (17.4 and 19.6 Å,

respectively), so that the asymmetric spin-density distribution in P^+ should not have a drastic effect on *D*. An upper limit to the value of $|D|$ for $P^+\Phi_A^-$ may be obtained by using eq 12 with *R* equal to the minimum edge-to-edge separation of the two porphyrin rings. This distance is 9.8 Å in *Rb. sphaeroides*, giving $D \simeq -30$ G. Of course the localization of spin density on the two radicals will never be as extreme as this, and *D* can be expected to be much nearer the −5 G value estimated earlier. As described above, such dipolar couplings have a negligible effect on the shape of the radical pair spectra.

An alternative explanation for an unexpectedly large dipolar coupling would be that the charge separated radical pair state had a substantially smaller center-to-center distance than the uncharged molecules in the crystal. Given the Coulombic attraction of the charges involved, a small contraction, perhaps of the order of 1 Å, would seem plausible. As far as we are aware there is no evidence for more dramatic rearrangements. Although not exactly comparable because of the larger separations involved, the spin-polarized EPR spectra of $P^+Q_A^-$[33] provide strong evidence that the charge separation induces no significant structural changes on the microsecond timescale of the experiment.

In short, our failure convincingly to simulate either the *Rps. viridis* or *Rb. sphaeroides* YW(M210) mutant spectra with a large value of $|D|$, together with the likelihood that $|D|$ is less than 10 G, strongly suggests that the shape of these spectra contain very little information on the dipolar coupling in $P^+\Phi_A^-$.

Line Shapes of $P^+\Phi_A^-$ Spectra. If the fine structure in the spin-polarized spectrum of *Rps. viridis* cannot be ascribed to a large dipolar interaction, then what is its origin? Clearly, interactions that are substantially smaller than the ∼68 G peak-to-peak separation will, like a −5 G dipolar coupling, have no perceptible effect on the lineshape. The *g*-anisotropy, although in principle the source of fine structure (cf. the much narrower spin-polarized spectra of $P^+Q_A^-$ [20,24−26,29,33,34]) is far too small in $P^+\Phi_A^-$.

The spectra of $P^+\Phi_A^-$ shown in Figures 4, 5, and 7 were obtained by subtracting the underlying polarized spectrum of ^{3}P. It is therefore important to examine this data-processing step as a possible source of spectral distortion. As described in ref 23, the EPR spectrum of ^{3}P, free from $P^+\Phi_A^-$ contributions, was recorded 1 μs after the light flash and was subtracted from the earlier spectra after suitable scaling. This procedure should work well if the shape of the ^{3}P spectrum is invariant over the period 100 ns to 1 μs. If this is not the case, then one can expect subtraction artefacts in the difference spectrum, which are likely to be most pronounced near the turning points of the ^{3}P spectrum, where the EPR signal is strongest. Careful inspection of the experimental ^{3}P spectra (not shown) reveals that there *are* indeed slight changes in the relative amplitudes and shapes of different parts of the triplet spectrum and that the shoulders in the *Rps. viridis* radical pair spectrum seem to be weaker at 150 ns than at 50 ns

The spectrum of the radical pair occupies the central portion of the much broader EPR spectrum of ^{3}P, and overlaps the Y peaks of the latter, which are separated by $|D(^3\mathrm{P})| - 3|E(^3\mathrm{P})|$, where $D(^3\mathrm{P})$ and $E(^3\mathrm{P})$ are the usual zero field splitting parameters. For *Rb. sphaeroides*, this separation is ∼100 G, so that the most prominent subtraction artefacts would be expected to lie *outside* the $P^+\Phi_A^-$ spectrum, whose peak-to-peak separation is only ∼40 G. Indeed, in some of the radical pair spectra of *Rb. sphaeroides*, small dips in the base line *can* be seen, shifted by approximately ±50 G with respect to the center of the spectrum. These glitches should not affect our interpretation of the *Rb. sphaeroides* spectrum. The radical pair EPR spectrum is sufficently strong at 100 ns (15−25% of the amplitude of the ^{3}P signal, see Figure 1 of ref 23) that the subtraction procedure itself is not expected to distort the radical pair signal.

The zero field splitting parameters of ^{3}P in *Rps. viridis* differ significantly from those of *Rb. sphaeroides*: in particular, the Y peaks are somewhat closer, with a separation of ∼50 G. These peaks now fall *between* the extrema of the radical pair spectrum. Indeed the Y peaks of ^{3}P seem to occur at about the same positions as the shoulders on the radical pair spectrum. It therefore seems possible that this fine structure may not reflect a large unidentified magnetic interaction in $P^+\Phi_A^-$, but rather slight subtraction artefacts arising from the processing of the EPR data. If this is indeed the case, then the values of k_T and *J* reported above, obtained by ignoring the shoulders, should be as reliable as those for *Rb. sphaeroides*, where no such problem arises.

The next question is whether the artefacts affect the radical pair spectrum of the *Rb. sphaeroides* YW(M210) mutant, whose Y peaks are separated by ∼110 G. These strong, relatively sharp features in the ^{3}P spectrum thus occur rather close to the positions of the outer pair of peaks in the mutant radical pair spectrum shown in Figure 7. Although much stronger than the shoulders seen for *Rps. viridis*, it seems possible that the errors involved in subtracting a 1 μs triplet spectrum from the earlier spectra might give rise to these strong features. If this is indeed so, then only the inner pair of AE peaks, separated by ∼30 G, would be genuine. Unfortunately, this part of the spectrum is too strongly overlapped to allow reliable values of k_T and *J* to be extracted.

The origin of the slight time dependence of the shape of the EPR spectrum is not clear. One possibility triplet−triplet energy transfer to carotenoid (Car) can be excluded. No transfer has been observed in *Rps. viridis*,[45] and although the spectrum of ^{3}Car does appear at higher temperatures in the M210 mutant, it is negligible at 30 K. An alternative possibility, that cannot be ruled out at this stage, is that a small amount of spin−lattice relaxation is distorting the ^{3}P intensities.

One solution to these problems would be to simulate the time dependence of the spin-polarized spectrum of ^{3}P so that subtraction of an independently recorded spectrum would not be necessary. This might have the added advantage of yielding extra information on the primary radical pair. For example, the singlet−triplet interconversion in $P^+\Phi_A^-$ should be anisotropic, by virtue of the dipolar coupling, so that different parts of the ^{3}P spectrum might be expected to have different polarizations and rise times. Such effects might allow one to estimate the dipolar interaction in $P^+\Phi_A^-$ and its orientation with respect to the zero-field splitting tensor of ^{3}P. These possibilities are under investigation.

Energetic Heterogeneity of $P^+\Phi_A^-$. Hitherto we have assumed that the three types of bacterial reaction center investigated each has unique values of the recombination rate constants and the exchange interaction. This simplification must be examined in the light of the finding of Ogrodnik et al.[46] that there is an energetic heterogeneity in $P^+\Phi_A^-$, which results in a spread of values of k_S, k_T, and *J*. This heterogeneity explains, at least qualitatively, the inconsistent values of k_T obtained from static magnetic field effects and from RYDMR spectra:[7] the amplitudes of the latter decrease rapidly with increasing k_T, making RYDMR insensitive to reaction centers with large k_T. The details of the inhomogeneous distributions of the three parameters are evidently very complex and much work will be needed to elucidate them. For the time being, certain assump-

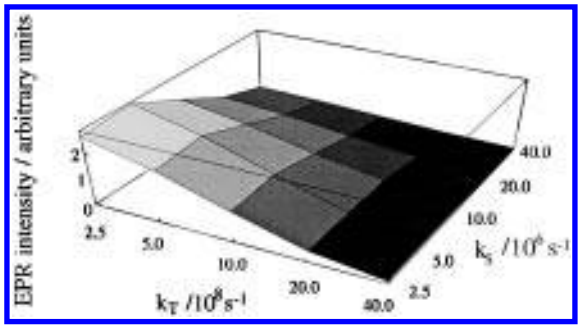

Figure 8. Calculated dependence of the EPR amplitude on k_S and k_T, for $J = -5$ G.

tions have to be made if any information is to be extracted from experimental measurements. It must be recognized that different experiments are inevitably sensitive to different parts of the various distributions and so give *weighted* average values of k_S, k_T, and J.

The EPR observations are restricted to the tail of the radical pair decay and so select those radical pairs with smaller than average recombination rate constants. The amplitude of the spectrum falls as both k_S and k_T are increased (Figure 8): larger k_S results in fewer radical pairs being present during the 100−200 ns period of the EPR measurement, while larger k_T gives broader and thus weaker spectra. However, the effect is not enormous: doubling both k_S and k_T simultaneously from the values found for *Rb. sphaeroides* causes a 5.3-fold reduction in the EPR signal. Thus, our values of k_S and k_T are undoubtedly underestimates of the mean values of the two distributions, but the error is unlikely to be gross unless the heterogeneity is substantial. The effects of the energetic heterogeneity of the two rates, which are coupled through superexchange, should be correlated.[46] The small values of k_S selected by the EPR experiment should belong to radical pairs which also have small k_T.

Similar arguments apply to the exchange interaction. As may be seen from Figure 4B, the predicted EPR amplitudes of $P^+\Phi_A^-$ become smaller as $|J|$ rises because of the increasing width of the signal. Once again, one can expect our values to be averages weighted towards the lower end of the distribution of $|J|$. If the distribution is "single-humped", e.g., Gaussian, the inclusion of the heterogeneity into the spectral simulations will lead to changes in linewidth and peak-to-peak separation. Only in the event of, for example, a double humped distribution, could structure of the kind seen for the *Rb. sphaeroides* YW(M210) mutant be expected.

The most comprehensive and accurate set of measurements of k_S, k_T, and J are those of Michel-Beyerle, Ogrodnik, and Volk for quinone-depleted *Rb. sphaeroides* R26 (and also for *Chloroflexus aurantiacus* and *Rb. capsulatus*).[7] In the temperature range 90−200 K, the singlet recombination rate constant, extracted from the effect of a static magnetic field on the average radical pair lifetime and the quantum yield of ^{3}P, is $\sim 2 \times 10^7$ s^{-1}; the triplet recombination rate, determined by RYDMR spectroscopy, is $\sim 6 \times 10^8$ s^{-1}; and the exchange interaction, also from RYDMR, is 5 ± 1 G. Both k_S and k_T have a small temperature dependence: k_S falls and k_T rises as the temperature is reduced from 200 to 90 K. Extrapolating to 70 K, the temperature of our EPR measurements on *Rb. sphaeroides*,[23] one obtains $k_S = (1.2 \pm 0.2) \times 10^7$ s^{-1} and $k_T = (11 \pm 1) \times 10^8$ s^{-1}. J is essentially independent of temperature: its sign can be inferred from the anisotropy of magnetic field effects, but the argument is somewhat involved and relies on estimates of the directions of the transition dipole moments for excitation and probing.[47,48] All these data were determined on the assumption of negligible energetic heterogeneity.

Our values of all three parameters for *Rb. sphaeroides* ($k_S = (1.2 \pm 0.3) \times 10^7$ s^{-1}, $k_T = (5.7 - 8.8) \times 10^8$, $|J| = 8 - 6$ G) agree well with the results of RYDMR experiments.[7,14,15] This correspondence presumably arises from the similar sensitivity of the two techniques to these parameters. RYDMR selects predominantly radical pairs with small k_T,[7] while the EPR measurements are biased toward small k_S, k_T, and $|J|$.

Our analysis of the *Rps. viridis* measurements gives somewhat different values: $k_S = (8 \pm 2) \times 10^7$ s^{-1}, $k_T = (6.5-10.0) \times 10^8$ s^{-1}, $-J = 17-16$ G. In particular, k_S and $|J|$ are significantly larger than for *Rb. sphaeroides*. The lack of previous measurements of these quantities makes it difficult to comment on their magnitudes, save to say that the difference may be related to the edge-to-edge separation of P^+ and Φ_A^-: 9.5 Å in *Rps. viridis*[43] and 9.8 Å in *Rb. sphaeroides*.[40] The faster singlet recombination and stronger exchange interactions in *Rps. viridis* should result in a lower ^{3}P yield: our calculations suggest a factor of ∼5 difference between the two bacteria. Unfortunately, the triplet yield in *Rps. viridis* seems not to have been measured.[7]

A further point should be made in respect of the *Rps. viridis* data. k_S is determined from the ∼10 ns rise time of ^{3}P (measured over the interval 10−50 ns) while k_T and J are derived from the EPR spectrum of $P^+\Phi_A^-$, averaged over the period 100−200 ns. If the kinetics are approximately monoexponential out to ∼100 ns, the 10 ns time constant implies that an undetectably tiny fraction of the radical pairs would survive until the start of the EPR measurement. This apparent contradiction may be taken to provide further evidence for strong heterogeneity in the kinetics of ^{3}P formation, i.e. a substantial fraction of $P^+\Phi_A^-$, say 10−20%, decays much more slowly than 10 ns. Such a spread of k_S values does not invalidate the determination of k_T and J because, as explained above, the shapes of the spectra are insensitive to k_S. Nor is it a problem for the interpretation of the *Rb. sphaeroides* data, where the (slower) radical pair decay and triplet formation were measured over the *same* time interval as the EPR spectra.

The samples of *Rb. sphaeroides* and *Rps. viridis* used for the EPR experiments[23] differ in that forward electron transfer was blocked in the former by extraction of Q_A and in the latter by reduction of Q_A. The presence of Q_A^- in *Rps. viridis* could, in principle, drastically reduce the lifetime of $P^+\Phi_A^-$ via the very rapid singlet−triplet interconversion that would be driven by the ∼140 G exchange interaction[49] between Φ_A^- and Q_A^-. Our calculations suggest a lifetime far smaller than the 10 ns observed: so small that there would be no detectable concentration of radical pairs remaining at 100 ns. It is possible that the spin-lattice relaxation of Q_A^-, which is part of a $[Fe^{2+}Q_A^-]$ complex, is so fast that Q_A^- is effectively decoupled from Φ_A^-. If so, then the differences between *Rps. sphaeroides* and *Rps. viridis* reflect genuine variations in k_S, k_T, and J rather than the presence or absence of Q_A^-.

It is clear from the model described above that a *negative* exchange interaction J is required to account for the AE polarization of $P^+\Phi_A^-$. In contrast, a *positive* sign is indicated by the electron spin polarization of the semiquinone Q_A^- in prereduced chromatophores of *Rhodospirillum rubrum* in which the magnetic interaction between Q_A^- and the Fe^{2+} was uncoupled by detergent treatment[19] and also in prereduced reaction centers of *Rb. sphaeroides* in which the Fe^{2+} was replaced by diamagnetic Zn^{2+}.[50] In addition, magnetic field effects on the yield of ^{3}P in *Rb. sphaeroides* 2.4.1 are consistent with a positive

J in Q_A-reduced wild-type reaction centers, but a negative *J* for the Q_A-depleted YW(M210) mutant.[51] Finally, the electron spin polarization of $P^+Q_A^-Fe^{2+}$ in *Rb. sphaeroides*, with different quinones as Q_A, also indicates $J > 0$.[20] One could argue that prereduction of Q_A (by freezing in the light in the presence of sodium ascorbate) inverted the sign of *J*, were it not for the AE polarization of $P^+\Phi_A^-$ in Q_A-reduced *Rb. sphaeroides*.[23] Conceivably the energetic heterogeneity[46] of $P^+\Phi_A^-$ might provide a resolution of this problem. Although it is clear that radical pairs with small k_S also have small k_T, it is difficult to see how *J* correlates with k_S and k_T. If the width of the inhomogeneous distribution of exchange interactions were broad enough to encompass both positive and negative values of *J* and if small k_S and k_T were to go hand-in-hand with negative *J*, while radical pairs with larger rate constants had positive *J*, then the various experiments mentioned above could yield different signs for *J* if they were sensitive to radical pairs with different lifetimes. This possibility clearly needs further investigation. Alternatively, the apparent discrepancies in the sign of *J* may be related to the relatively harsh detergent treatment.[19,50]

5. Summary

In the preceding paragraphs, we have obtained values for the singlet and triplet recombination rate constants and the exchange interaction in the primary radical pair in photosynthetic bacterial reaction centers on the assumption that the heterogeneity of these quantities is negligible. The kinetics of the formation of ^3P are dominated by k_S, while the transient $P^+\Phi_A^-$ EPR spectrum is controlled by the magnitudes of both k_T and *J* and the sign of *J*. This neat separation, which allows all three parameters to be extracted, is possible for two reasons. First $k_T \gg k_S$, so that the lifetime broadening of the spectra has little contribution from k_S. Second, the experimental measurements of the ^3P kinetics are most sensitive to reaction centers with lifetimes comparable to k_S^{-1}, i.e., those with small Q and slow singlet−triplet interconversion rates.

The EPR experiments discussed here provide a source of information on exchange interactions and recombination rates that compliments measurements of magnetic field effects on $P^+\Phi_A^-$ lifetimes and ^3P quantum yields. EPR observations of $P^+\Phi_A^-$ are sensitive to the tail of the radical pair decay and so select from the inhomogeneous distribution of $P^+\Phi_A^-$ those radical pairs with small recombination rate constants. In this respect EPR is similar to RYDMR. EPR also gives an average exchange interaction for $P^+\Phi_A^-$ weighted toward the lower end of the distribution of $|J|$. Nanosecond time-resolved measurements of static magnetic field effects, by contrast, give less biased averages for k_S, k_T, and *J*.[7] However, the latter involve experiments in zero or weak applied fields and can only be interpreted using semiclassical,[52] one-proton,[9] or equivalent approximations for the singlet−triplet mixing produced by hyperfine interactions. The EPR experiments, like RYDMR, use fields much stronger than any magnetic interaction within the radical pair, and so can be analysed without the need for such simplifying assumptions. To realize the full potential of the EPR approach, however, more extensive measurements of spectra and kinetics, as well as of their temperature dependence, will be needed.[53]

Acknowledgment. We are grateful to Susana Shochat for preparing the *Rb. sphaeroides* YW(M210) mutant, to Romano Kroemer and Jonathan Jones for expert computational assistance, and Martin Volk for a useful discussion. U.T. is supported in part by an EPSRC research studentship. A.J.H. acknowledges the support of the Netherlands Foundation for Chemical Research (SON), financed by the Netherlands Organisation for Scientific Research (NWO). I.I.P. and I.B.K. are grateful to the NWO for financial support (Grant 0730036/047-013-036).

References and Notes

(1) Warshel, A.; Creighton, S.; Parson, W. *J. Phys. Chem.* **1988**, *92*, 2696.
(2) Michel-Beyerle, M. E.; Plato, M.; Deisenhofer, J.; Michel, H.; Bixon, M.; Jortner, J. *Biochim. Biophys. Acta* **1988**, *932*, 52.
(3) Plato, M.; Möbius, K.; Michel-Beyerle, M. E.; Bixon, M.; Jortner, J. *J. Am. Chem. Soc.* **1988**, *110*, 7279.
(4) Friesner, R. A.; Won, Y. *Biochim. Biophys. Acta* **1989**, *977*, 99.
(5) Scherer, P. O. J.; Fischer, S. F. *Chem. Phys.* **1989**, *131*, 115.
(6) Bixon, M.; Jortner, J.; Michel-Beyerle, M. E. *Biochim. Biophys. Acta* **1991**, *1056*, 301.
(7) Volk, M.; Ogrodnik, A.; Michel-Beyerle, M. E. *Anoxygenic Photosynthetic Bacteria*; Blankenship, R. E., Madigan, M. T., Bauer, C. E., Eds.; Kluwer: Dordrecht, 1995, p 595.
(8) Werner, H.-J.; Schulten, K.; Weller, A. *Biochim. Biophys. Acta* **1978**, *502*, 255.
(9) Haberkorn, R.; Michel-Beyerle, M. E. *Biophys. J.* **1979**, *26*, 489.
(10) Salikhov, K. M.; Molin, Yu. N.; Sagdeev, R. Z.; Buchachenko, A. L. *Spin Polarization and Magnetic Field Effects in Radical Reactions*; Elsevier: Amsterdam, 1984.
(11) Steiner, U.; Ulrich, T. *Chem. Rev.* **1989**, *89*, 51.
(12) Bowman, M. K.; Budil, D. E.; Closs, G. L.; Kostka, A. G.; Wraight, C. A.; Norris, J. R. *Proc. Natl. Acad. Sci. U.S.A.* **1981**, *78*, 3305.
(13) Norris, J. R.; Bowman, M. K.; Budil, D. E.; Tang, J.; Wraight, C. A.; Closs, G. L. *Proc. Natl. Sci. U.S.A.* **1982**, *79*, 5532.
(14) Moehl, K. W.; Lous, E. J.; Hoff, A. J. *Chem. Phys. Lett.* **1985**, *121*, 22.
(15) Hunter, D. A.; Hoff, A. J.; Hore, P. J. *Chem. Phys. Lett.* **1987**, *134*, 6.
(16) Lersch, W.; Michel-Beyerle, M. E. *Advanced EPR. Applications in Biology and Biochemistry*; Hoff, A. J., Ed.; Elsevier: Amsterdam, 1989; p 685.
(17) Hoff, A. J.; Hore, P. J. *Chem. Phys. Lett.* **1984**, *108*, 104.
(18) Hore, P. J. *Advanced EPR. Applications in Biology and Biochemistry*; Hoff, A. J., Ed.; Elsevier: Amsterdam, 1989; p 405.
(19) Hore, P. J.; Riley, D. J.; Semlyen, J. J.; Zwanenburg, G.; Hoff, A. J. *Biochim. Biophys. Acta* **1993**, *1141*, 221.
(20) Morris, A. L.; Snyder, S. W.; Zhang, Y.; Tang, J.; Thurnauer, M. C.; Dutton, P. L.; Robertson, D. E.; Gunner, M. R. *J. Phys. Chem.* **1995**, *99*, 3854.
(21) Bixon, M.; Jortner, J.; Michel-Beyerle, M. E. *Z. Phys. Chem.* **1993**, *180*, 193.
(22) Bixon, M.; Jortner, J.; Michel-Beyerle, M. E. *Chem. Phys.* **1995**, *197*, 389.
(23) Proskuryakov, I. I.; Klenina, I. B.; Hore, P. J.; Bosch, M. K.; Gast, P.; Hoff, A. J. *Chem. Phys. Lett.* **1996**, *257*, 333.
(24) Hore, P. J.; Hunter, D. A.; McKie, C. D.; Hoff, A. J. *Chem. Phys. Lett.* **1987**, *137*, 495.
(25) Closs, G. L.; Forbes, M. D. E.; Norris, J. R. *J. Phys. Chem.* **1987**, *91*, 3592.
(26) Stehlik, D.; Bock, C. H.; Petersen, J. *J. Phys. Chem.* **1989**, *93*, 1612.
(27) At temperatures above about 100 K, there is some recombination to the excited state P* of the primary donor: k_S should then be regarded as the sum of the rate constants of the two singlet recombination pathways.
(28) Till, U.; Hore, P. J. *Mol. Phys.* **1997**, *90*, 289.
(29) Feick, R.; Martin, J. L.; Volk, M.; Scheidel, G.; Langenbacher, T.; Urbano, C.; Ogrodnik, A.; Michel-Beyerle, M. E. *Reaction Centers of Photosynthetic Bacteria*; Michel-Beyerle, M. E., Ed.; Springer-Verlag: Berlin, 1990; p 181.
(30) McElroy, J. D.; Feher, G.; Mauzerall, D. C. *Biochim. Biophys. Acta* **1972**, *267*, 363.
(31) Okamura, M. Y.; Isaacson, R. A.; Feher, G. *Biochim. Biophys. Acta* **1979**, *546*, 394.
(32) McElroy, J. D.; Mauzerall, D. C.; Feher, G. *Biophys. Biochim. Acta* **1974**, *333*, 261.
(33) van der Est, A.; Bittl, R.; Abresch, C. E.; Lubitz, W.; Stehlik, D. *Chem. Phys. Lett.* **1993**, *212*, 561.
(34) van den Brink, J. S.; Hulsebosch, R. J.; Gast, P.; Hore, P. J.; Hoff, A. J. *Biochemistry* **1994**, *33*, 13688.
(35) Zwanenburg, G.; Hore, P. J. *Chem. Phys. Lett.* **1993**, *203*, 65.
(36) Bittl, R.; Kothe, G. *Chem. Phys. Lett.* **1991**, *177*, 547.
(37) Kothe, G.; Weber, S.; Bittl, R.; Ohmes, E.; Thurnauer, M. C.; Norris, J. R. *Chem. Phys. Lett.* **1991**, *186*, 474.
(38) Kothe, G.; Weber, S.; Ohmes, E.; Thurnauer, M. C.; Norris, J. R. *J. Phys. Chem.* **1994**, *98*, 2706.

(39) Bittl, R.; van der Est, A.; Kamlowski, A.; Lubitz, W.; Stehlik, D. *Chem. Phys. Lett.* **1994**, *226*, 349.

(40) Entry 4RCR in the Protein Data Bank at Brookhaven National Laboratory.

(41) Klette, R.; Törring, J. T.; Plato, M.; Möbius, K.; Bönigk, B.; Lubitz, W. *J. Phys. Chem.* **1993**, *97*, 2015.

(42) Shochat, S.; Artl, T.; Francke, C.; Gast, P.; van Noort, P. I.; Otte, S. C. M.; Schelvis, H. P. M.; Schmidt, S.; Vijgenboom, E.; Vrieze, J.; Zinth, W.; Hoff, A. J. *Photosynth. Res.* **1994**, *40*, 55.

(43) Entry 1PRC in the Proton Data Bank at Brookhaven National Laboratory.

(44) Lendzian, F.; Huber, M.; Isaacson, R. A.; Endeward, B.; Plato, M.; Bönigk, B.; Möbius, K.; Lubitz, W.; Feher, G. *Biochim. Biophys. Acta* **1993**, *1183*, 139.

(45) Holton, D.; Windsor, M. W.; Parson, W. W.; Thornber, J. P. *Biochim Biophys. Acta* **1978**, *501*, 112.

(46) Ogrodnik, A.; Keupp, W.; Volk, M.; Aumeier, G.; Michel-Beyerle, M. E. *J. Phys. Chem.* **1994**, *98*, 3432.

(47) Chidsey, C. E. D.; Kirmaier, C.; Holten, D.; Boxer, S. G. *Biochim. Biophys. Acta* **1984**, *766*, 424.

(48) Ogrodnik, A.; Lersch, W.; Michel-Beyerle, M. E.; Deisenhofer, J.; Michel, H. *Antenna and Reaction Centers of Photosynthetic Bacteria*; Michel-Beyerle, M. E., Ed.; Springer-Verlag: Berlin, 1985; p 198.

(49) Prince, R. C.; Tiede, D. M.; Thornber, J. P.; Dutton, P. L. *Biochim. Biophys. Acta* **1977**, *462*, 467.

(50) Bosch, M.; Gast, P.; Franken, E. M.; Zwanenburg, G.; Hore, P. J.; Hoff, A. J. *Biochim. Biophys. Acta* **1996**, *1276*, 106.

(51) van der Vos, R.; Franken, E. M.; Sexton, S. J.; Shochat, S.; Gast, P.; Hore, P. J.; Hoff, A. J. *Biochim. Biophys. Acta* **1995**, *1230*, 51.

(52) Schulten, K.; Wolynes, P. G. *J. Chem. Phys.* **1978**, *68*, 3292.

(53) Preliminary calculations of the dynamics of radical pair recombinations in plant photosystem II, where k_S appears to be considerably smaller than in *Rb. sphaeroides* (Volk, M. Personal communication), suggest that all three parameters (k_S, k_T, and J) affect both the spectra and the kinetics. Nevertheless, it should be possible to derive values of the parameters if signals can be observed.